

Identification of Conserved Pappalysin 1-Derived Circular RNA-Mediated Competing Endogenous RNA in Osteosarcoma

Guang-Fu Ming*, Bo-Hua Gao* and Peng Chen^{id}

Department of Orthopedics, Hainan General Hospital (Hainan Affiliated Hospital of Hainan Medical University), Haikou, China.

Evolutionary Bioinformatics
Volume 17: 1–9
© The Author(s) 2021
Article reuse guidelines:
sagepub.com/journals-permissions
DOI: 10.1177/11769343211041379



ABSTRACT: The etiology of osteosarcoma (OS) is complex and not fully understood till now. This study aimed to identify the miRNAs, circRNAs, and genes (mRNAs) that are differentially expressed in OS cell lines to investigate the mechanism of circRNA-associated competing endogenous RNAs (ceRNAs) in OS. Microarray datasets reporting mRNA (GSE70414), miRNA (GSE70367), and circRNA changes (GSE96964) in human OS cell lines were downloaded, differentially expressed (DE) RNAs were identified, and DEmRNAs were used for the annotation of Gene Ontology (GO) biological processes (BP), and Kyoto Encyclopedia of Genes and Genomes (KEGG) pathways. The mechanisms of DEcircRNA-mediated ceRNAs were identified in a step-by-step process. A total of 326 DEmRNAs, 45 DEmiRNAs, and 110 DEcircRNAs were identified from 3 datasets. The DEmRNAs were associated with GO BP terms, including cholesterol biosynthetic process, angiogenesis, extracellular matrix organization and KEGG pathways, including p53 signaling pathway and biosynthesis of antibiotics. The final ceRNA network consisted of 8 DEcircRNAs, including 5 pappalysin (PAPPA) 1-derived DEcircRNAs (hsa_circ_0005456, hsa_circ_0088209, hsa_circ_0002052, hsa_circ_0088214 and has_circ_0008792, all downregulated), 3 DEmiRNAs (hsa-miR-760, hsa-miR-4665-5p and hsa-miR-4539, all upregulated), and downregulated genes (including MMP13 and HMOX1). The ceRNA regulation network of OS was built, which played important roles in the pathogenesis of OS and might be of great importance in therapy.

KEYWORDS: Osteosarcoma, human osteosarcoma cell lines, competing endogenous RNA, pappalysin 1

RECEIVED: March 15, 2021. **ACCEPTED:** August 3, 2021.

TYPE: Original Research

FUNDING: The author(s) received no financial support for the research, authorship, and/or publication of this article.

DECLARATION OF CONFLICTING INTERESTS: The author(s) declared no potential conflicts of interest with respect to the research, authorship, and/or publication of this article.

CORRESPONDING AUTHOR: Peng Chen, Department of Orthopedics, Hainan General Hospital (Hainan Affiliated Hospital of Hainan Medical University), 19 Xiuhua Road, Xiuying District, Haikou 570000, China. Email: a15508968968@163.com

Introduction

Osteosarcoma (OS) is a primary bone malignancy with a higher incidence in both children and older individuals.^{1,2} The overall 5-year survival rate is approximately 65% and <25% in patients with metastasis²⁻⁴ and 0% in those with pulmonary metastasis.⁵

The etiology of OS is complex and not fully understood till now. It has been reported that there is vast tumor heterogeneity in patients with OS.⁶ The commonly used OS-derived cell lines, including U2OS, U2OS/MTX300, HOS, MG63, 143B, ZOS and ZOSM, serve vital roles in understanding the pathogenesis and therapeutic responses of OS and are used as conventional 2D models. Cell lines reflect only a part of the subtypes of tumors and cannot cover the tumor heterogeneity and full genetic spectrum of the primary OS.⁷⁻⁹ Most anticancer drugs in cell lines are ineffective in clinical research, which restricts drug screening, personalized therapy, and the survival of patients. However, the application of conventional 2D models has invaluable roles in improving the understanding of the pathogenesis, drug screening, and therapeutic responses in tumors. Moreover, the integration of more than 1 cell line in preclinical research might suggest the typical etiology, homogeneity, and common therapeutic responses. Previous research has shown that changes in the combination of chemotherapy drugs and the method of administration cannot improve the 5-year survival rate, even if

the dose is increased.¹⁰ Therefore, the discovery of biomarkers related to the treatment of OS is of great significance.

The genetic and epigenetic alterations in protein-coding mRNAs and non-coding RNAs, including microRNAs (miRNAs), long non-coding RNAs (lncRNAs) and circular RNAs (circRNAs), serve crucial roles in the pathogenesis, development, drug, and therapy response, and recurrence of tumors. Compared with genes, miRNAs, lncRNAs, and circRNAs participate in and modulate tumor etiology and development indirectly through their targets or competing endogenous RNA (ceRNA) mechanism.¹¹⁻¹⁴ For instance, Song and Li¹⁴ reported that circ_0001564 regulated the proliferation and apoptosis of OS cells and cell lines via sponging miR-29c-3p. Zhang et al showed that circRNA ubiquitin-associated protein 2 promoted OS progression via sponging miR-143. The characterization of circRNA-associated ceRNA in OS has been widely studied. However, the consistency and integrated analysis of circRNA-associated ceRNAs in OS cell lines have not been well reported until now.

We performed this present study using microarray dataset of OS cell lines. The miRNAs, circRNAs, and genes (mRNAs) that are differentially expressed in >5 OS cell lines were identified and retained in the analysis of circRNA-associated ceRNA in OS. This study might provide novel insights into the pathogenesis or therapeutic treatments in OS concerning circRNA-associated ceRNA and maybe offer new insight for the development of OS drugs.

* Guang-Fu Ming and Bo-Hua Gao are co-first authors.



Materials and Methods

Microarray data

Microarray datasets reporting the mRNA (GSE70414), miRNA (GSE70367) and circRNA changes (GSE96964) in human OS cell lines were obtained from the National Center for Biotechnology Information Gene Expression Omnibus database (<https://www.ncbi.nlm.nih.gov/>). GSE70414 (Affymetrix Human Genome U133 Plus 2.0 Array) and GSE70367 datasets (GPL16384 (miRNA-3) Affymetrix Multispecies miRNA-3 Array) show the mRNA and miRNA changes in 5 OS cell lines including HOS, MG63, HY, Saos and Hu09 relative to human mesenchymal stem cells (hMSCs). GSE96964 dataset (GPL19978 Agilent-069978 Arraystar Human CircRNA microarray V1) presents the circRNA profiles in 7 human OS cell lines including U2OS, U2OS/MTX300, HOS, MG63, 143B, ZOS and ZOSM compared with human osteoblasts hFOB1.19.

Data processing and differentially expressed RNA (DERNA) identification

The GEL files derived from all 3 datasets were downloaded and processed using the Affy package (GSE70414 and GSE70367, version 1.52.0, <http://bioconductor.org/help/search/index.html?q=affy>)¹⁵ or Limma package (GSE96964; version 3.10.3, <http://www.bioconductor.org/packages/2.9/bioc/html/limma.html>).¹⁶ Microarray datasets were preprocessed for background correction and quantile normalization. The expression of related RNAs was calculated. The average value (expression value) was calculated, while multiple probes were mapped to the same RNA (mRNA/miRNA/circRNA) and used as the expression level.

Differential expression analysis of RNAs was performed using Bayesian approach methods in the Limma package.¹⁷ DERNAs (DEmRNAs, DEmiRNAs and DEcircRNAs) in OS cell lines and controls were identified following the thresholds of the P -value $< .05$ and $|\log_2FC$ (fold change) ≥ 1 . Hierarchical clustering analyzes of DERNAs were performed using R package pheatmap (version 1.0.8, <https://cran.r-project.org/package=pheatmap>) and presented as clustering heatmaps.

Enrichment analysis

The online tool Database for Annotation, Visualization and Integrated Discovery (version 6.8; <https://david.ncifcrf.gov/>)¹⁸ was employed to identify the Gene Ontology (GO) biological processes (BP) and Kyoto Encyclopedia of Genes and Genomes (KEGG) pathways^{19,20} that were significantly associated with DEmRNAs (P -value $\leq .05$ and number of enriched genes count ≥ 2) in OS cell lines and controls.

DEmiRNA-mRNA regulatory network construction

Due to the large number of DEmiRNAs, the difference threshold was further screened, and DEmiRNAs with $|\log_2FC| \geq 2$

were included in the subsequent prediction analysis. Before the construction of the miRNA-mRNA regulatory network, we predicted the targets of DEmiRNAs in miRWalk, miRanda, miRDB, miRMap, Pictar2, RNA22 and TargetScan using miRWalk2.0 (<http://zmf.umm.uni-heidelberg.de/apps/zmf/mirwalk2/>).²¹ The overlapping genes between the predictions of targets at least in 5 databases and DEmRNAs were identified as potential targets of DEmiRNAs. The DEmRNAs in the miRNA-mRNA regulatory network were used in the KEGG pathway enrichment analysis using clusterProfiler (version 2.4.3, <http://bioconductor.org/packages/3.2/bioc/html/clusterProfiler.html>).²² The miRNA-mRNA regulatory network was visualized using Cytoscape (version 3.2.0, <http://www.cytoscape.org/>).²³

CeRNA regulatory network construction

The DEmiRNAs in the aforementioned miRNA-mRNA regulatory network were listed, and all DEcircRNA IDs were converted to standard names. The FASTA files of these DEmiRNAs and DEcircRNAs were extracted and processed using miRanda (version 3.3a, <https://omictools.com/miranda-tool>)²⁴ to identify the circRNA-miRNA interaction pairs. Interaction pairs with interaction score ≥ 150 and energy < -30 were retained and used in the construction of the ceRNA regulatory network using Cytoscape. The overlapped DEmiRNAs between the circRNA-miRNA and miRNA-mRNA regulatory networks were identified, and the associated DEcircRNAs and DEmRNAs were used in the construction of the ceRNA regulatory network using Cytoscape. The circRNA-associated genes and locations were predicted using CircInteractome (<https://circinteractome.nia.nih.gov/index.html>).

Drug-gene interaction prediction

DEmRNAs in the circRNA-miRNA-mRNA regulatory network were identified and used in the selection of potential therapeutic drugs. Drug-gene associations were identified in Drug-Gene Interaction Database 3.0 (DGIdb 3.0, <http://www.dgldb.org/>) (default parameters),²⁵ and the document-proven relationship pairs were screened to build the drug-gene associations. Finally, drug-gene associations were visualized using Cytoscape.

Results

Summary of DERNAs

After normalization, a total of 326 DEmRNAs (76 upregulated and 250 downregulated), 45 DEmiRNAs (24 upregulated and 21 downregulated), and 110 DEcircRNAs (8 upregulated and 102 downregulated) were differentially expressed in the OS cell lines in GSE70414, GSE70367 and GSE96964 datasets, respectively (Figure 1A). The clustering heatmap of these DERNAs in each dataset is shown in Figure 1B. Enrichment analysis for the DEmRNAs in GSE70367 showed that there were 8 GO BP terms associated with

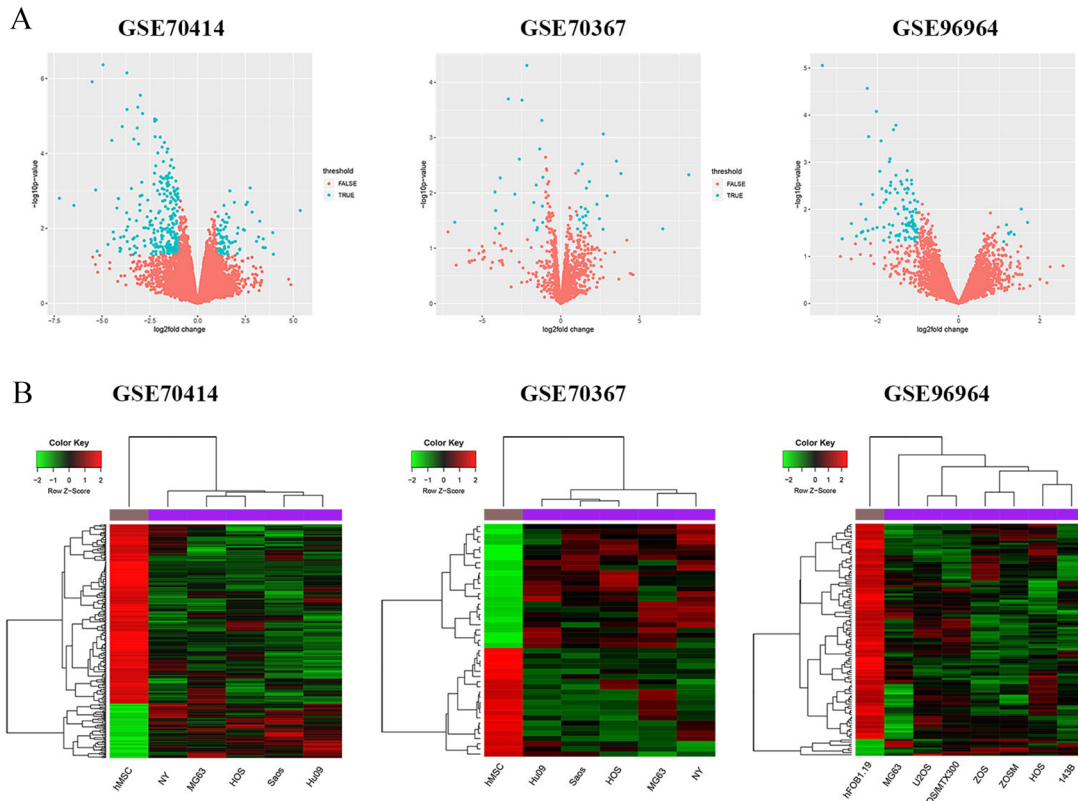


Figure 1. Summary of the differentially expressed RNAs (DERNAs) in human OS cell lines. (A) Volcano plot of the DEmRNAs, DE miRNAs, and DE circRNAs in OS cell lines versus controls (hMSCs or hFOB1.19). Blue and red dots indicate DERNAs and non-significantly differentially expressed RNAs, respectively. X- and Y-axis represent \log_2FC and $-\log_{10}P$ -value of expression changes, respectively. (B) Clustering heatmaps of DERNAs. Green and red indicate down- and upregulation, respectively.

upregulated DEmRNAs and downregulated DEmRNAs were enriched in 57 GO BP terms (GO:0006695 cholesterol biosynthetic process, GO:0001525 angiogenesis, and GO:0030198 extracellular matrix organization) and 4 KEGG pathways (hsa04115:p53 signaling pathway and hsa01130: biosynthesis of antibiotics) (Figure 2). Figure 2 shows the top 8 or 10 GO BP terms and all KEGG pathways.

Construction of the DE miRNA-mRNA regulatory network

Before the construction of DE miRNA-mRNA regulatory network, we selected 20 DE miRNAs (9 upregulated and 11 downregulated) with $|\log_2FC| \geq 2$ between OS cell lines and hMSCs in GSE70367 due to a large number of candidate DE miRNAs ($n=45$). Then, a total of 136 target mRNAs of these 20 DE miRNAs, covered by DEmRNAs in GSE70414, were predicted from 7 databases. Finally, the overlapping genes between target genes of 20 DE miRNAs and DEmRNAs were acquired. The corresponding DE miRNA-mRNA regulatory network consisted of 294 miRNA-mRNA pairs (lines) (Figure 3). The top 20 DEmRNAs and all DE miRNAs in this network are presented in Table 1. About 19 DE miRNAs (8 upregulated and 11 downregulated) and 136 DEmRNAs (31 upregulated and 105 downregulated) (Table S1).

Based on the DEmRNAs in the DE miRNA-mRNA regulatory network, the KEGG pathways associated with these DE miRNAs in the network were identified. We found that hsa-miR-1292-5p was associated with the “Notch signaling pathway”; hsa-miR-1270, hsa-miR-543, and hsa-miR-758-3p were associated with “mucin-type O-glycan biosynthesis”; hsa-miR-4539 was related to “C-type lectin receptor signaling pathway” and “viral carcinogenesis”; hsa-miR-4665-5p was enriched in the “IL-17 signaling pathway” and “relaxin signaling pathway” (Figure 4).

Construction of the ceRNA network

The interaction between all DE circRNAs in GSE96964 and the aforementioned 19 DE miRNAs in the DE miRNA-mRNA regulatory network was predicted using miRanda. About 9 DE circRNA-miRNA pairs were identified (Table 2), including 3 upregulated DE miRNAs, 1 upregulated DE circRNA, and 7 downregulated DE circRNAs. All ceRNA-DE miRNA pairs are shown in Table S2. Then, the DE circRNAs and DEmRNAs regulated by 3 upregulated DE miRNAs (hsa-miR-4665-5p, hsa-miR-760, and hsa-miR-4539) were identified, and the subsequent ceRNA network was comprised of 9 circRNA-miRNA and 28 miRNA-mRNA pairs (Figure 5). ceRNA pairs of hsa_circ_0088737/0005456/0088209/has-miR-4665-5p/

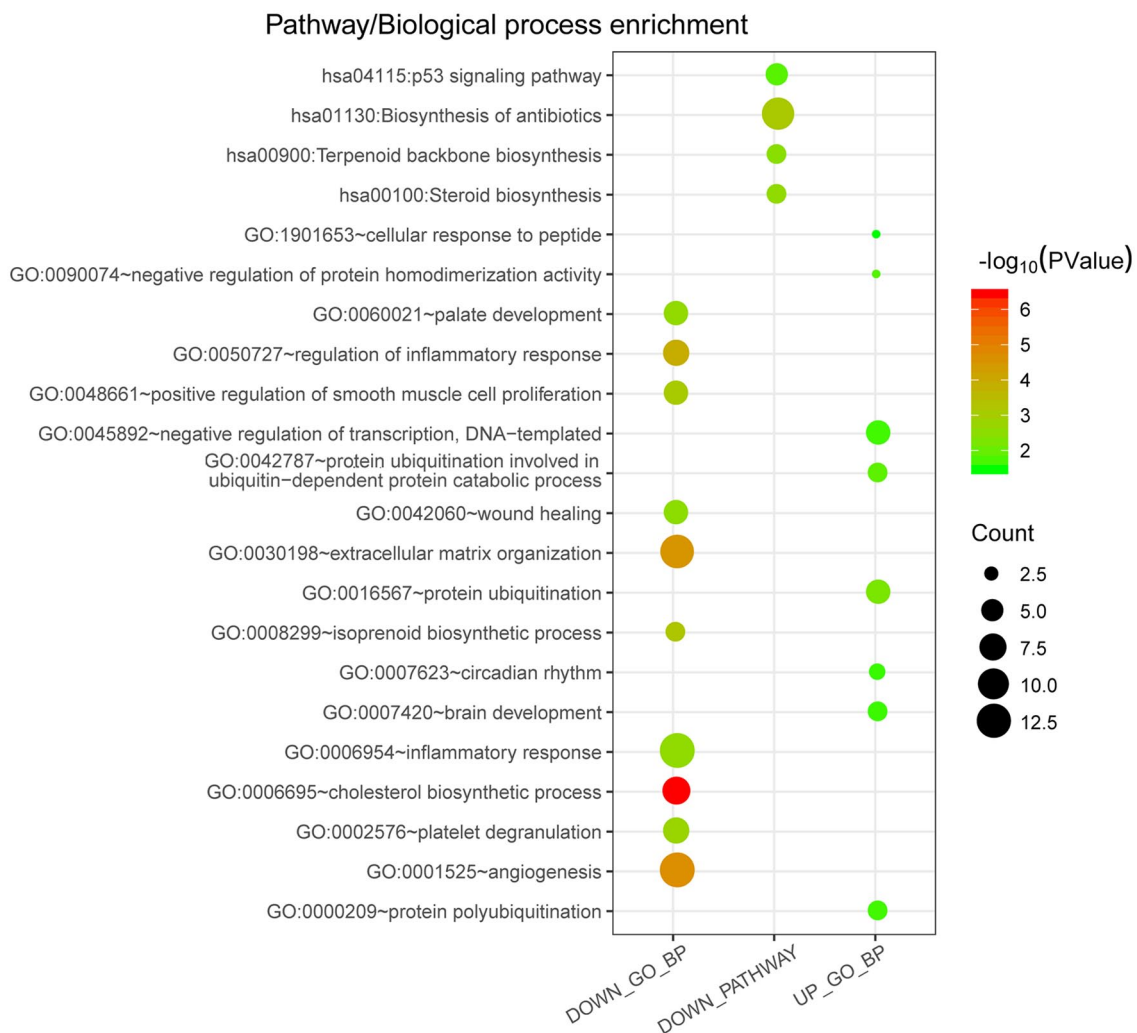


Figure 2. The pathways and biological processes (BPs) associated with differentially expressed mRNAs (DEmRNAs) in GSE70414. Bubble size indicates gene number. The higher the gene number, the larger the bubble diameter. Red and green indicate high and low values of $-\log_{10}(P\text{-value})$, respectively.

collagenase-3 (MMP13), hsa_circ_0064136/has-miR-4539/early growth response 2 (EGR2)/Cep85, and hsa_circ_0088209/0002052/0088214/0008792/has-miR-760/heme oxygenase-1 (HMOX1)/transforming growth factor (TGF)- β -stimulated clone 22 domain 3 (TSC22D3) were identified. We found the hsa_circ_0088209, hsa_circ_0088214, hsa_circ_0008792, hsa_circ_0002052, and hsa_circ_0005456 are located in chr9, and its associated gene is pappalysin 1 (PAPPA) (Table 2), suggesting that these circRNAs were derived from the same gene PAPPA. hsa_circ_0032462, hsa_circ_0088737, and hsa_circ_0064136 are associated with signal-induced proliferation-associated 1-like 1 (SIPA1L1), CDKN1A interacting zinc finger protein 1 (CIZ1), and SET domain containing 5 (SETD5), respectively.

Prediction of drug-gene association

The 26 DEmRNAs in the ceRNA network were then employed in the drug prediction in DGIdb 3.0. About 6 down-regulated DEmRNAs (MMP13, HMOX1, and EGR2) were targeted by 26 chemicals (Figure 6), including 3-methylpyridine, sorafenib, aspirin, biliverdin, sunitinib, and tretinoin.

MMP13 might be a target of 3-methylpyridine, marimastat, and other chemicals. HMOX1 was targeted by sorafenib, aspirin, biliverdin, sunitinib, formic acid, and zinc chloride. Both EGR2 and TSC22D3 were targeted by tretinoin and dexamethasone, respectively.

Discussion

ceRNA has been a novel mechanism for exploring the interactions of RNA. For example, mRNA, miRNA and circRNA were known as the RNA interaction molecules, which have important biological significance.²⁶ Previous research has reported that the ceRNA was associated with the molecular mechanism of cancers, such as breast cancer,²⁷ glioblastoma,²⁸ and lung cancer.²⁹ Our study performed an integrated analysis of circRNA-associated ceRNAs in >5 OS cell lines. We confirmed that they have similar characteristics with miRNAs, circRNAs, and genes in OS cell lines, including HOS, MG63, HY, Saos, Hu09, U2OS and 143B. In our research, regarding the parameter settings, we set $P\text{-value} < .05$ and $|\log_2FC| \geq 1$ to screen for DERNAs, but we have obtained a large number of DE miRNAs, so we further set

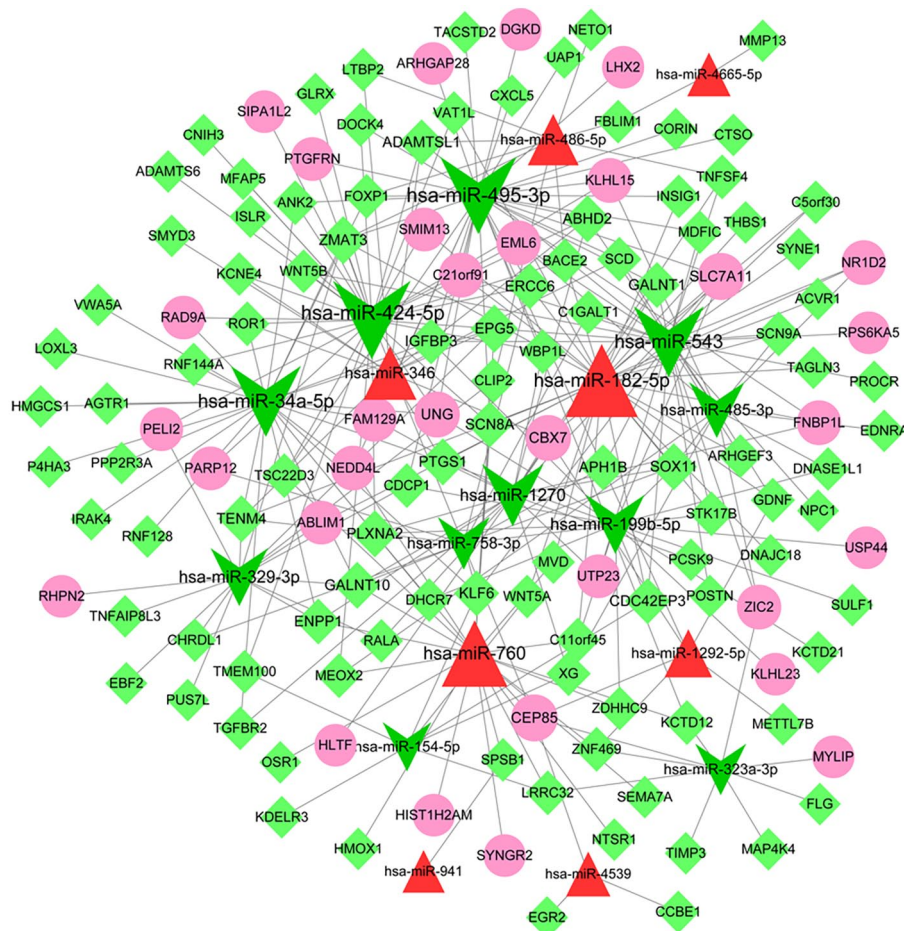


Figure 3. Differentially expressed (DE) miRNA-mRNA regulatory network. Green arrows and red triangles represent down- and upregulated DEMiRNAs, respectively. Pink circles and green prisms represent up- and down-regulated DEmRNAs, respectively.

$|\log_2FC| \geq 2$ to screen for DEMiRNAs; and in the DEMiRNA-mRNA regulatory network construction section, we predicted the targets of DEMiRNAs at least in 5 databases, compared with some studies,³⁰ we used relatively more databases, which can provide us with more accurate results. After rounds of selection, we identified that hsa_circ_0088737, hsa_circ_0005456, hsa_circ_0088209, hsa_circ_0002052, hsa_circ_0088214, and hsa_circ_0008792 played vital roles in OS pathogenesis by regulating miR-4665-5p, miR-4539, and miR-760.

Hsa_circ_0088209 is located in chr9 (118949432-118997916), and its associated gene symbol is PAPPA. The interactions of hsa_circ_0088209 (downregulated), and 4 other PAPPA-derived DEcircRNAs (hsa_circ_0088214, hsa_circ_0008792, hsa_circ_0002052, and hsa_circ_0005456) with hsa-miR-4665-5p and/or hsa-miR-760 (both upregulated) were identified in OS cell lines. Our present study suggested that both hsa-miR-4665-5p and hsa-miR-760 were upregulated in OS cell lines compared with hMSCs, while all PAPPA-derived DEcircRNAs were downregulated in OS cell lines. These revealed the potential circRNA-mediated ceRNA via sponging upregulated hsa-miR-4665-5p and hsa-miR-760 in OS cell lines.

Previous research has proved that hsa-miR-760 is upregulated in ovarian cancer, and its overexpression promotes the proliferation and aggressiveness of ovarian cancer cells and is associated with poor prognosis.³¹ Research has found that hsa-miR-760 is upregulated in hepatocellular carcinoma, and it could serve as a potential prognostic miRNAs of hepatocellular carcinoma.²⁶ However, it has been proved that hsa-miR-760 is downregulated in non-small cell lung cancer, and its expression suppresses the proliferation and metastasis of cells and enhances sensitivity to TNF-related apoptosis-inducing ligand.^{32,33} These results suggested heterogeneity in tumor pathogenesis. Our present study demonstrated that the upregulation of both hsa-miR-4665-5p and hsa-miR-760 in OS cell lines compared with hMSCs might suggest the promotion of hsa-miR-4665-5p and hsa-miR-760 overexpression in OS progression.

Our study demonstrated that both hsa-miR-4665-5p and hsa-miR-760 (both upregulated) were targeted by PAPPA-derived DEcircRNAs, including hsa_circ_0088214, hsa_circ_0008792, hsa_circ_0002052, and hsa_circ_0005456 in OS cell lines. PAPPA, also known as pregnancy-associated plasma protein-A, is an oncogenic metalloproteinase that promotes the growth and invasion of human cancers, including lung cancer, ovarian cancer, and Ewing sarcoma.³⁴⁻³⁷ PAPPA is lowly

Table 1. The differentially expressed (DE) miRNAs and top 19 DEMRNAs in the DE miRNA-mRNA regulatory network.

DEMIRNAS	DESCRIPTION	DEGREE	DEMRNAS	DESCRIPTION	DEGREE
hsa-miR-424-5p	Down	34	ZMAT3	Down	6
hsa-miR-495-3p	Down	33	EPG5	Down	6
hsa-miR-182-5p	Up	29	TENM4	Down	5
hsa-miR-34a-5p	Down	27	SOX11	Down	5
hsa-miR-543	Down	27	PTGS1	Down	5
hsa-miR-760	Up	23	PLXNA2	Down	5
hsa-miR-1270	Down	19	GALNT10	Down	5
hsa-miR-199b-5p	Down	16	ABHD2	Down	5
hsa-miR-329-3p	Down	15	SLC7A11	Up	5
hsa-miR-485-3p	Down	13	CEP85	Up	5
hsa-miR-346	Up	11	ADAMTSL1	Down	4
hsa-miR-758-3p	Down	10	APH1B	Down	4
hsa-miR-323a-3p	Down	9	CBX7	Up	4
hsa-miR-486-5p	Up	9	CDC42EP3	Down	4
hsa-miR-154-5p	Down	7	ENPP1	Down	4
hsa-miR-1292-5p	Up	6	ERCC6	Down	4
hsa-miR-4539	Up	3	GALNT1	Down	4
hsa-miR-4665-5p	Up	2	IGFBP3	Down	4
hsa-miR-941	Up	1	KLF6	Down	4
			SCN8A	Down	4

expressed in normal tissues and highly expressed in bone cells for bone formation during fetal development. PAPPa cleaves insulin-like growth factor (IGF) binding proteins (IGFBPs), promotes the separation of IGFs from IGF-IGFBP complex, and thus activates the IGF pathway.³⁶ The oncogenic roles of PAPPa are mediated by the activation of the NF- κ B,³⁸ TGF- β ,³⁹ PI3K/AKT, and ERK signaling pathways.⁴⁰ Our present study showed that the HMOX1, which is upregulated in various human solid tumors, was a target of hsa-miR-760 and several anticancer drugs, including sorafenib and sunitinib. These DEcircRNAs in OS might suggest that PAPPa was involved in the pathogenesis of OS and potential circRNA-associated ceRNA via sponging upregulated hsa-miR-4665-5p and hsa-miR-760 in OS cell lines.

MMP13 is a predicted target of hsa-miR-4665-5p and is associated with bone formation via regulation by the transcription factor gene Cbfa1 and involvement of TGF- β . The upregulation of hsa-miR-4665-5p was associated with melatonin-mediated anticancer properties in breast and prostate cancers.^{41,42} Hirahata et al⁴³ reported that a higher frequency of pulmonary metastasis was observed in cases with MMP13-positive OS than MMP13-negative OS. The expression of MMP13 in human cancers

promotes cancer cell invasion and metastasis and is correlated with poor outcomes.⁴³⁻⁴⁶ These studies showed that the expression of MMP13 was crucial in cancer invasion and metastasis, while the inhibition or deletion of MMP13 suppressed the development and metastasis of tumors.⁴⁴⁻⁴⁶ Our present study suggested that the expression of MMP13 was downregulated in all OS cell lines compared with hMSCs. MMP13 was only targeted by upregulated hsa-miR-4665-5p in the ceRNA network. The upregulated hsa-miR-4665-5p and downregulated MMP13 in OS might suggest different tumorigenesis or antitumor properties of hsa-miR-4665-5p/MMP13 axis. Moreover, the MMP13-marimastat interaction might show potential therapeutic value of marimastat use in OS treatment.

Conclusions

In conclusion, we found that 5 downregulated PAPPa-derived DEcircRNAs, including hsa_circ_0088209, hsa_circ_0088214, hsa_circ_0008792, hsa_circ_0002052, and hsa_circ_0005456, may play crucial roles in the pathogenesis and treatment of OS. Moreover, the ceRNA regulation network of OS was built, which provided novel insights into the pathogenesis of OS and might be of great importance in the therapy of OS.

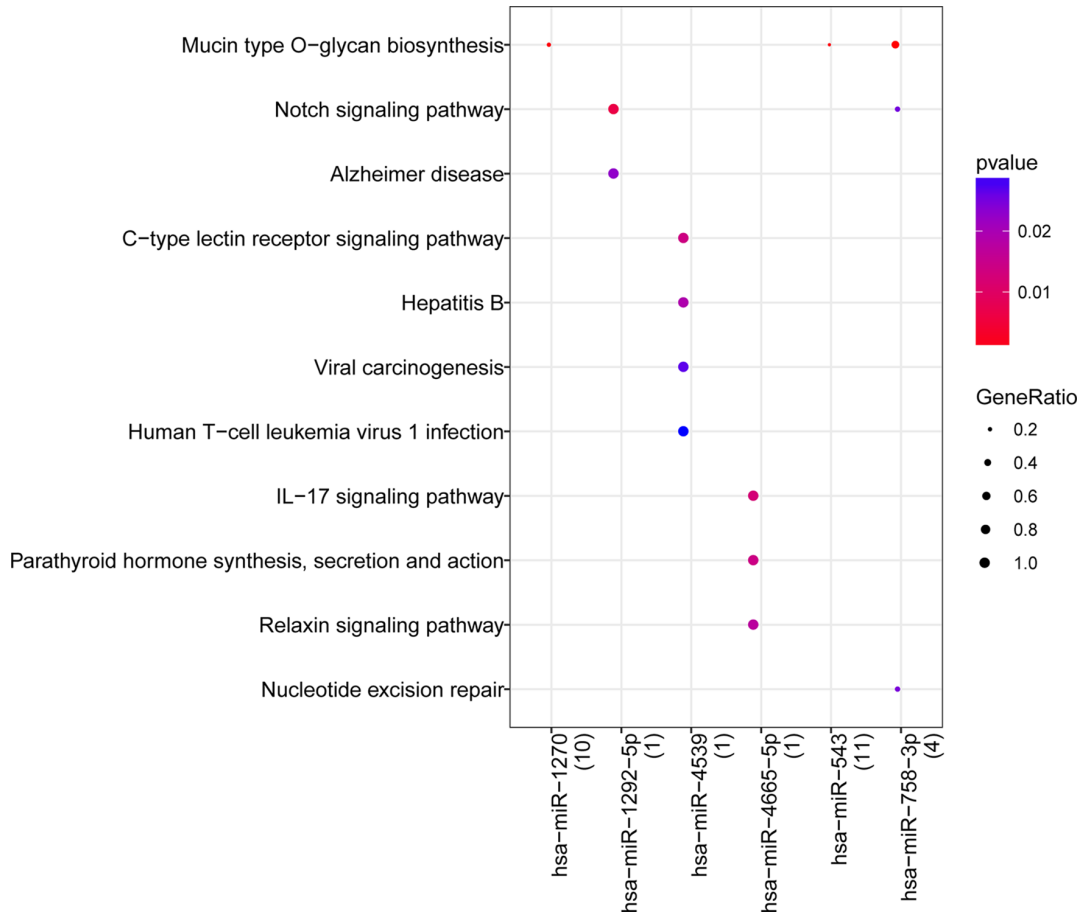


Figure 4. Kyoto Encyclopedia of Genes and Genomes (KEGG) pathways associated with differentially expressed miRNAs (DEmiRNAs) in the miRNA-mRNA regulatory network. The horizontal axis indicates the miRNA number, the vertical axis indicates the entry name, the dot size represents the miRNA number, and the color represents significance. The redder the color, the greater the importance.

Table 2. The predicted interaction pairs of differentially expressed (DE) circRNAs and miRNAs.

MIRNA	UP/DOWN	CIRCRNA	UP/DOWN	GENE SYMBOL	LOCATION	SCORE	ENERGY
hsa-miR-760	Up	hsa_circ_0088209	Down	PAPPA	chr9:118949432-118997916	449	-73.23
hsa-miR-4665-5p	Up	hsa_circ_0088209	Down	PAPPA	chr9:118949432-118997916	433	-77.48
hsa-miR-760	Up	hsa_circ_0088214	Down	PAPPA	chr9:118969734-118989831	301	-50.44
hsa-miR-760	Up	hsa_circ_0008792	Down	PAPPA	chr9:118969734-119033695	301	-50.44
hsa-miR-760	Up	hsa_circ_0002052	Down	PAPPA	chr9:118969734-118997916	301	-50.44
hsa-miR-4665-5p	Up	hsa_circ_0005456	Down	PAPPA	chr9:118949432-118950495	289	-54.12
hsa-miR-4665-5p	Up	hsa_circ_0032462	Up	SIPA1L1	chr14:72054287-72090953	284	-45.66
hsa-miR-4665-5p	Up	hsa_circ_0088737	Down	CIZ1	chr9:130931330-130943078	282	-47.18
hsa-miR-4539	Up	hsa_circ_0064136	Down	SETD5	chr3:9482139-9506356	163	-32.53

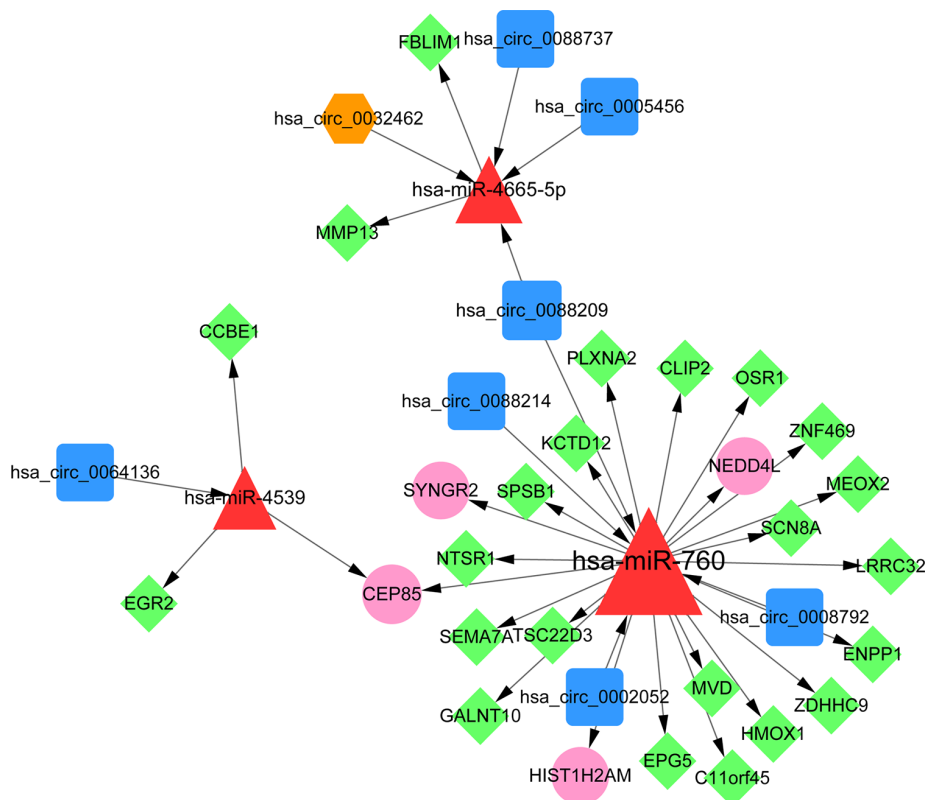


Figure 5. The ceRNA regulatory network of circRNA-miRNA-mRNA. Red triangles represent upregulated differentially expressed miRNAs (DEmiRNAs). Pink circles and green prisms represent up- and down-regulated DEmRNAs, respectively. Orange hexagon and blue squares indicate up- and down-regulated DEcircRNAs, respectively.

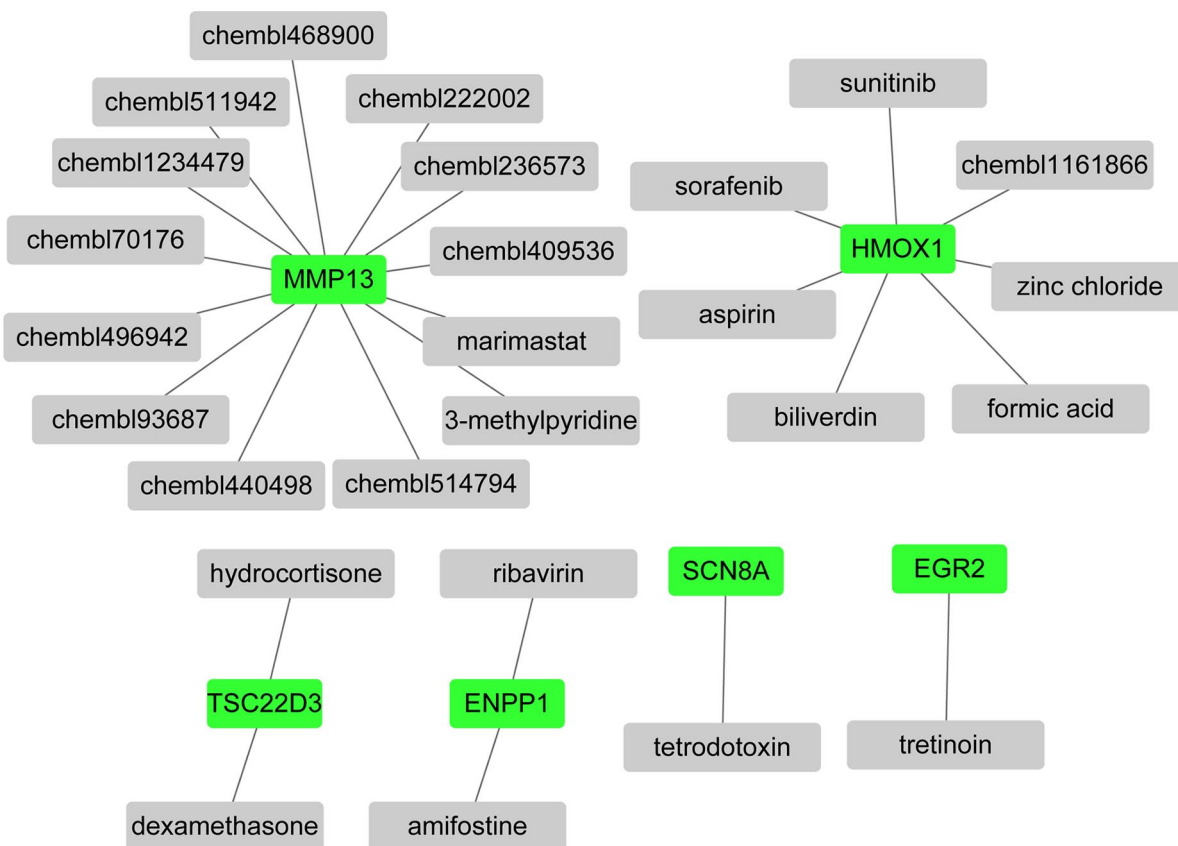


Figure 6. Drug-gene interactions. Green and gray squares represent downregulated mRNAs and chemicals, respectively.

Author Contributions

GM and PC were responsible for the conception and design of the research, and drafting the manuscript. BG performed the data acquisition, data analysis and interpretation. GM, PC, and BG participated in the design of the study and performed the statistical analysis. All authors read and approved the final manuscript. Authors contributed equally to this work.

Ethical Statement

The authors are accountable for all aspects of the work in ensuring that questions related to the accuracy or integrity of any part of the work are appropriately investigated and resolved.

ORCID iD

Peng Chen  <https://orcid.org/0000-0002-0466-1303>

Supplemental Material

Supplemental material for this article is available online.

REFERENCES

- Zheng S, Qiao G, Min D, et al. Heterogeneous expression and biological function of ubiquitin carboxy-terminal hydrolase-L1 in osteosarcoma. *Cancer Lett.* 2015;359:36-46.
- Lindsey BA, Markel JE, Kleinerman ES. Osteosarcoma overview. *Rheumatol Ther.* 2017;4:25-43.
- Ottaviani G, Jaffe N. The epidemiology of osteosarcoma. In: Jaffe N, Bruland OS, Bielack SS, eds. *Pediatric and Adolescent Osteosarcoma*. Springer; 2010: 3-13.
- Felix M, Guyot MC, Isler M, et al. Endothelin-1 (ET-1) promotes MMP-2 and MMP-9 induction involving the transcription factor NF- κ B in human osteosarcoma. *Clin Sci.* 2006;110:645-654.
- Ward WG, Mikaelian K, Dorey F, et al. Pulmonary metastases of stage IIB extremity osteosarcoma and subsequent pulmonary metastases. *J Clin Oncol.* 1994;12:1849-1858.
- Scott MC, Tomiyasu H, Garbe JR, et al. Heterotypic models of osteosarcoma recapitulate tumor heterogeneity and biological behavior. *Dis Model Mech.* 2016;9:1435-1444.
- Stein WD, Litman T, Fojo T, Bates SE. A serial analysis of gene expression (SAGE) database analysis of chemosensitivity: comparing solid tumors with cell lines and comparing solid tumors from different tissue origins. *Cancer Res.* 2004;64:2805-2816.
- Szakacs G, Gottesman MM. Comparing solid tumors with cell lines: implications for identifying drug resistance genes in cancer. *Mol Interv.* 2004;4:323-325.
- Seim I, Jeffery PL, Thomas PB, Nelson CC, Chopin LK. Whole-genome sequence of the metastatic PC3 and LNCaP human prostate cancer cell lines. *Genes Genomes Genet.* 2017;7:1731-1741.
- Li S, Sun W, Wang H, Zuo D, Hua Y, Cai Z. Research progress on the multi-drug resistance mechanisms of osteosarcoma chemotherapy and reversal. *Tumour Biol.* 2015;36:1329-1338.
- Liu Y, Ye LI, Liu J, Yuntao WU, Zhu Q. MicroRNA-132 inhibits cell growth and metastasis in osteosarcoma cell lines possibly by targeting Sox4. *Int J Oncol.* 2015;47:1672-1684.
- Wang Y, Zhang Y, Yang T, et al. Long non-coding RNA MALAT1 for promoting metastasis and proliferation by acting as a ceRNA of miR-144-3p in osteosarcoma cells. *Oncotarget.* 2017;8:59417-59434.
- Kun-Peng Z, Xiao-Long M, Lei Z, Chun-Lin Z, Jian-Ping H, Tai-Cheng Z. Screening circular RNA related to chemotherapeutic resistance in osteosarcoma by RNA sequencing. *Epigenomics.* 2018;10:1327-1346.
- Song YZ, Li JF. Circular RNA hsa_circ_0001564 regulates osteosarcoma proliferation and apoptosis by acting miRNA sponge. *Biochem Biophys Res Commun.* 2018;495:2369-2375.
- Gautier L, Cope L, Bolstad BM, Irizarry RA. affy—analysis of *Affymetrix GeneChip* data at the probe level. *Bioinformatics.* 2004;20:307-315.
- Smyth GK. limma: linear models for microarray data. In: Gentleman R, Carey VJ, Huber W, Irizarry RA, Dudoit S, eds. *Bioinformatics and Computational Biology Solutions Using R and Bioconductor*. Springer New York; 2005:397-420.
- Ritchie ME, Phipson B, Wu D, et al. limma powers differential expression analyses for RNA-sequencing and microarray studies. *Nucleic Acids Res.* 2015;43:e47.
- Lempicki RA. Systematic and integrative analysis of large gene lists using DAVID bioinformatics resources: abstract. *Nat Protoc.* 2008;4:44-57.
- The Gene Ontology Consortium. Gene Ontology Consortium: going forward. *Nucleic Acids Res.* 2015;43(D1):D1049-D1056.
- Kanehisa M, Sato Y, Kawashima M, Furumichi M, Tanabe M. KEGG as a reference resource for gene and protein annotation. *Nucleic Acids Res.* 2016;44(D1):D457-D462.
- Dweep H, Gretz N. miRWalk2.0: a comprehensive atlas of microRNA-target interactions. *Nat Methods.* 2015;12:697.
- Yu G, Wang L-G, Han Y, He Q-Y. clusterProfiler: an R package for comparing biological themes among gene clusters. *OMICS.* 2012;16:284-287.
- Shannon P, Markiel A, Ozier O, et al. Cytoscape: a software environment for integrated models of biomolecular interaction networks. *Genome Res.* 2003;13:2498-2504.
- Enright AJ, John B, Gaul U, Tuschl T, Sander C, Marks DS. MicroRNA targets in *Drosophila*. *Genome Biol.* 2003;5:R1.
- Cotto KC, Wagner AH, Feng Y-Y, et al. DGIdb 3.0: a redesign and expansion of the drug-gene interaction database. *Nucleic Acids Res.* 2018;46(D1):D1068-D1073.
- Zhang X, Ma L, Zhai L, et al. Construction and validation of a three-microRNA signature as prognostic biomarker in patients with hepatocellular carcinoma. *Int J Med Sci.* 2021;18:984-999.
- Li Z, Yang HY, Dai XY, et al. CircMETTL3, upregulated in a m6A-dependent manner, promotes breast cancer progression. *Int J Biol Sci.* 2021;17:1178-1190.
- Rahnama S, Bakhshinejad B, Farzam F, Bitaraf A, Ghazimoradi MH, Babashah S. Identification of dysregulated competing endogenous RNA networks in glioblastoma: a way toward improved therapeutic opportunities. *Life Sci.* 2021;277:119488.
- Wei D, Sun L, Feng W. hsa_circ_0058357 acts as a ceRNA to promote non-small cell lung cancer progression via the hsa-miR-24-3p/AVL9 axis. *Mol Med Rep.* 2021;23(6):470.
- Jin X, Guan Y, Sheng H, Liu Y. Crosstalk in competing endogenous RNA network reveals the complex molecular mechanism underlying lung cancer. *Oncotarget.* 2017;8:91270-91280.
- Liao Y, Deng Y, Liu J, et al. MiR-760 overexpression promotes proliferation in ovarian cancer by downregulation of PHLPP2 expression. *Gynecol Oncol.* 2016;143:655-663.
- Yan C, Zhang W, Shi X, Zheng J, Jin X, Huo J. MiR-760 suppresses non-small cell lung cancer proliferation and metastasis by targeting ROS1. *Environ Sci Pollut Res.* 2018;25:18385-18391.
- Zhang X, Wang L, Liu Y, Huang W, Cheng D. MiR-760 enhances TRAIL sensitivity in non-small cell lung cancer via targeting the protein FOXA1. *Biomed Pharmacother.* 2018;99:523-529.
- Hong P, Sayaka H, Jun Z, Li M, Mark Zhi-Qing M. Protein secretion is required for pregnancy-associated plasma protein-A to promote lung cancer growth in vivo. *PLoS One.* 2012;7:e48799.
- Heitzeneder S, Sotillo E, Shern JF, et al. Pregnancy-associated plasma protein-A (PAPP-A) in Ewing sarcoma: role in tumor growth and immune evasion. *J Natl Cancer Inst.* 2019;111:970-982.
- Guo Y, Bao Y, Guo D, Yang W. Pregnancy-associated plasma protein A in cancer: expression, oncogenic functions and regulation. *Am J Cancer Res.* 2018;8:955-963.
- Becker MA Jr, Haluska P, Bale LK, Oxvig C, Conover CA. A novel neutralizing antibody targeting pregnancy-associated plasma protein-A inhibits ovarian cancer growth and ascites accumulation in patient mouse tumorgrafts. *Mol Cancer Ther.* 2015;14:973-981.
- Engelmann JC, Amann T, Ott-Rötzer B, et al. Causal modeling of cancer-stromal communication identifies PAPP-A as a novel stroma-secreted factor activating NF κ B signaling in hepatocellular carcinoma. *PLoS Comput Biol.* 2015;11:e1004293.
- Conover CA. Key questions and answers about pregnancy-associated plasma protein-A. *Trends Endocrinol Metab.* 2012;23:242-249.
- Yoshiko T, Hiroshi K, Mika S, Yasuyuki H, Naohiro K, Toshihiko T. Genetic downregulation of pregnancy-associated plasma protein-A (PAPP-A) by bikunin reduces IGF-I-dependent Akt and ERK1/2 activation and subsequently reduces ovarian cancer cell growth, invasion and metastasis. *Int J Cancer.* 2004;109:336-347.
- Lee SE, Kim SJ, Youn J-P, Seung Yong H, Cheung-Seog P, Seek PY. MicroRNA and gene expression analysis of melatonin-exposed human breast cancer cell lines indicating involvement of the anticancer effect. *J Pineal Res.* 2011;51:345-352.
- Sohn EJ, Won G, Lee J, Lee S, Kim SH. Upregulation of miRNA3195 and miRNA374b mediates the anti-angiogenic properties of melatonin in hypoxic PC-3 prostate cancer cells. *J Cancer.* 2015;6:19-28.
- Hirahata M, Osaki M, Kanda Y, et al. PAI-1, a target gene of miR-143, regulates invasion and metastasis by upregulating MMP-13 expression of human osteosarcoma. *Cancer Med.* 2016;5:892-902.
- Ou B, Zhao J, Guan S, et al. CCR4 promotes metastasis via ERK/NF- κ B/MMP13 pathway and acts downstream of TNF- α in colorectal cancer. *Oncotarget.* 2016;7:47637-47649.
- Mendonsa AM, Vansaun MN, Alessandro U, Piston DW, Fingleton BM, David Lee G. Host and tumor derived MMP13 regulate extravasation and establishment of colorectal metastases in the liver. *Mol Cancer.* 2015;14:1-12.
- Datar I, Feng J, Qiu X, et al. RKIP inhibits local breast cancer invasion by antagonizing the transcriptional activation of MMP13. *PLoS One.* 2015;10:e0134494.